J Appl Biomed
DOI: 10.32725/jab.2023.019

journal homepage: http://jab.zsf.jcu.cz

Journal of Applied Biomedicine

Original research article

Homospisulosine induced apoptosis in cervical carcinoma cells is associated with phosphorylation of Bcl-2 and up-regulation of p27/Kip1

Martina Bago Pilátová [1, a], Natália Nosálová [1, a], Gabriela Očkajáková [1], Martin Kello [1] *, Klaudia Kotorová [1], Peter Takáč [2], Peter Petik [3], Peter Bohuš [3], Kvetoslava Stanková [4], Miroslava Martinková [4], Roman Mezencev [5, b]

[1] *Pavol Jozef Šafárik University, Faculty of Medicine, Department of Pharmacology, Košice, Slovak Republic*
[2] *University of Veterinary Medicine and Pharmacy, Department of Pharmacology and Toxicology, Košice, Slovak Republic*
[3] *Pavol Jozef Šafárik University, Faculty of Medicine, Department of Pathology, Košice, Slovak Republic*
[4] *Pavol Jozef Šafárik University, Faculty of Science, Department of Organic Chemistry, Institute of Chemical Sciences, Košice, Slovak Republic*
[5] *Georgia Institute of Technology, School of Biological Sciences, Atlanta, GA, USA*

Abstract
Spisulosine (1-deoxysphinganine) is a sphingoid amino alcohol isolated from the sea clams that showed potent antiproliferative activity against a broad spectrum of solid tumors but failed in clinical trials due to neurotoxicity. However, its structural similarity to other bioactive sphingoids, interesting mode of action, and appreciable potency against cancer cells make it a suitable lead for future anticancer drug development. The present study was conducted to elucidate mechanisms of the antiproliferative/cytotoxic effects of newly synthesized spisulosine analog homospisulosine (KP7). The evaluation was performed on cervical carcinoma cells, representing an *in vitro* model of one of the most common cancer types and a significant worldwide cause of women's cancer mortality. Treatment with homospisulosine (2.0 μM) for 24, 48, and 72 h significantly inhibited the growth of HeLa cells *in vitro* and induced apoptosis detectable by DNA fragmentation, externalization of phosphatidylserine, dissipation of mitochondrial membrane potential, activation of caspase-3 and cleavage of PARP. In addition, treating HeLa cells with spisulosine increased p27 and Bcl-2 on protein levels and phosphorylation of Bcl-2 on Ser70 residue. These results support the potential for spisulosine analogs represented here by homospisulosine for future therapeutic development.

Keywords: Apoptosis; Cancer; Ceramide; Homospisulosine; Marine; Sphingoid bases; Sphingosine-1-phosphate; Spisulosine

Highlights:
- Homospisulosine is a new analog of a marine natural product, spisulosine.
- Homospisulosine inhibits the proliferation of various cancer cells.
- Homospisulosine showed pro-apoptotic potential on HeLa cells.
- Homospisulosine altered expression of apoptosis and proliferation-associated proteins including Bcl-2 family, p21, p27, CDC2, AKT.
- Homospisulosine is suitable for future drug development.

Introduction

Despite progress in cancer diagnosis and new therapeutic development, malignancies are still the second most frequent cause of death in industrially developed countries. Conventional chemotherapy can be very effective for some patients; however, it is often associated with toxicity that can result in serious adverse effects that reduce the quality of a patient's life and impede treatment continuation. This fact and efforts to enhance the effectiveness of cancer therapy have inspired scientific teams to look for new compounds with novel mechanisms of action, lower toxicity, increased safety, and better therapeutic response.

For thousands of years, natural products have played an essential role in treating and preventing diseases, including cancer. Many anticancer agents used in clinics are of natural origin or derived from natural products from various sources, such as plants, animals, and microorganisms, including those of marine origin (Baird et al., 2009; Roginsky et al., 2005).

* **Corresponding author:** Martin Kello, Pavol Jozef Šafárik University, Faculty of Medicine, Department of Pharmacology, 040 11 Košice, Slovak Republic; e-mail: martin.kello@upjs.sk
http://doi.org/10.32725/jab.2023.019
[a] These authors contributed equally to this article as first authors; [b] Senior author.

Submitted: 2023-05-11 • Accepted: 2023-11-09 • Prepublished online: 2023-11-28
J Appl Biomed 21/4: 218–227 • EISSN 1214-0287 • ISSN 1214-021X

The oceans and seas are essential food sources for humans, and their marine life is also a rich source of new and almost entirely unexplored compounds. Marine natural products display huge structural diversity and a range of diverse biological activities. Therefore, isolating new molecules from marine biota is an essential strategy for discovering new therapeutic agents, including anticancer agents. Molluscs represent 23% of marine organisms, and their secondary metabolites show a wide range of biological activities, including antibacterial, anti-inflammatory, antioxidant, and anticancer.

Spisula polynyma (Stimpson surf clam or Atlantic surf clam) is an edible clam harvested off the coast of Japan by the local population and used under the name "hokkigai" for the preparation of sushi (Den Brok et al., 2005, 2006; Haefner, 2003). This clam is a natural source of (+)-spisulosine, an amino alcohol of the sphingoid class (Rinehart et al., 2000). Spisulosine was shown to suppress the growth of cell lines *in vitro*, representing a broad spectrum of solid tumors, such as colon, ovary, breast, lung, kidney, liver, stomach, and melanoma, with IC_{50} values ranging from 20 to 200 nmol/l (Jimeno et al., 2004; Schöffski et al., 2011). Because of its potent inhibitory effects on cancer cells, structural similarity to other biologically active sphingoids, and its ability to induce apoptotic cell death through an unusual mode of action (Salcedo et al., 2007), spisulosine (ES-285) entered a phase I clinical trial in patients with advanced solid tumors (Sánchez et al., 2008; Singh et al., 2008). However, despite initially promising results, it failed in this indication and was discontinued due to adverse drug-related effects, the most prominent of which were neurotoxicity and hepatotoxicity (Rios et al., 2009; Salcedo et al., 2007; Vilar et al., 2012). To develop new spisulosine analogs with potentially more favorable toxicity profiles, we synthesized homospisulosine (KP7) (Stanková et al., 2015), evaluated its antiproliferative/cytotoxic activity, and investigated its anticancer mode of action, which is presented in this paper.

Materials and methods

Tested compound KP7 (homospisulosine): (3S,4R)-3-aminonadecan-4-ol was prepared in a stereoconvergent manner from 3,5-di-O-benzyl-d-xylofuranose, according to previously reported procedures (Stanková et al., 2015). Mass spectrometry and ^{1}H, ^{13}C NMR, and IR spectroscopy were used to confirm the structure, and the compound was subsequently dissolved in dimethyl sulfoxide (DMSO) with a final DMSO concentration in the culture medium lower than 0.2% that exhibited no cytotoxicity.

Cell cultures

HeLa (93021013, human cervical adenocarcinoma) were procured from the European Collection of Authenticated Cell Cultures (Salisbury, UK) and grown in RPMI 1640 medium (Biosera, Kansas City, MO, USA) in a humidified atmosphere containing 5% CO_2 at 37 °C. The growth medium was supplemented with a 10% fetal bovine serum (FBS), penicillin (100 IU/ml), and streptomycin (100 μg/ml) (all Invitrogen, Carlsbad, CA, USA). Cell viability, estimated by trypan exclusion, was greater than 95% before each experiment.

MTT assay

The colorimetric MTT assay, measuring metabolic activity as an indicator of cell proliferation and cytotoxicity, was used to study the effect of KP7. The cells were seeded at density 5×10^3 cells/well in 96-well polystyrene microplates (SARSTEDT, Nümbrecht, Germany). Twenty-four hours after cell seeding, various concentrations (0.5, 1, 5, 10 μM) of KP7 were added to cells. After 72 h of incubation, 10 μl of MTT (5 mg/ml) was added to each well and incubated for an additional 4 h at 37 °C in 5% CO_2, during which insoluble formazan was produced. The amount of tetrazolium dye MTT 3-(4,5-dimethylthiazol-2-yl)-2,5-diphenyltetrazolium bromide reduced to formazan was proportional to the number of viable cells (Mosmann, 1983). Adding 100 μl of 10% sodium dodecyl sulfate to each well and incubating for another 12 h allowed the formazan to be dissolved. The absorbance was measured at 540 nm using the automated uQuantTM Universal Microplate Spectrophotometer (Biotek, Winooski, VT, USA). The measured values were shown as a percentage of metabolic activity of the cells relative to unaffected control, which amounted to 100%. Dose-response modeling was performed using GraphPad Prism 8.0.1 using Hill's model for normalized response with variable slope. The IC_{50} value was determined as the concentration of KP7 required to reduce the number of viable cells to 50% of the control-treated cells.

Flow cytometric analysis

HeLa cells (1×10^6) were treated with KP7 at 2 μM concentration for 24, 48, and 72 hours. Floating and adherent cells were harvested, washed in PBS, and used for analysis. For intracellular staining, cells were fixated by 4% paraformaldehyde (15 min), followed by washing and permeabilization with 0.5% TWEEN 15 min RT, and stained according to the analysis and manufacturer's instructions (Table 1). Fluorescence was detected after 15–30 min of incubation at room temperature in the dark by a BD FACSCalibur flow cytometer (Becton-Dickinson, San Jose, CA, USA). Cell cycle distribution was determined by deconvolution of DNA content histograms, after discrimination of doublets (FL-2-W vs FL-2-A) and other cellular aggregates by Flow Jo 10.0 software (Tree Star, Inc., Ashland, OR, USA) using the Dean-Jett-Fox Model. A minimum of 1×10^4 cells was analyzed per analysis.

RNA isolation, cDNA synthesis, and Quantitative Real-Time PCR (qRT-PCR)

Total RNA was isolated from HeLa cells using TRI Reagent (Molecular Research Center, Inc., Cincinnati, OH, USA) according to the manufacturer's instructions. The quality of total RNA was verified on an agarose gel. Total RNA (0.5 μg) was reverse transcribed into cDNA by the RevertAid™ H Minus First Strand cDNA synthesis kit (Fermentas GmbH, St. Leon-Rot, Germany) according to the manufacturer's instruction and used for quantitative real-time PCR. The qRT-PCR analysis was performed in the ABI 7500 fast RTPCR system using iQTM SYBR Green Supermix (Bio-Rad Laboratories, USA) to verify the alterations in *PI3KCA* (PI3K), *AKT, MAPK14* (p38), *NFKBIA* (IκB), *BCL2, BCL2L1* (Bcl-XL), *BAX, APAF1, CASP3, CASP7, CDK2, CDKN1A* (p21), *CDKN1B* (p27), and reference *ACTB* (β-actin) genes expression. The PCR program was initiated after 5 min at 95 °C prior to 40 thermal cycles, each lasting at 95 °C for 15 s, at 60 °C for 10 s, and at 72 °C for 30 s (primer sequences were obtained from the RTPrimerDB database (Lefever et al., 2009) and listed in Table 2). The qRT-PCR data were analyzed using a comparative threshold (Ct) method, and the fold inductions of samples were compared with the untreated samples. β-actin was used as an internal reference gene to normalize the expression of the target genes. Melting curves for each PCR reaction were generated to ensure the purity of the amplification product.

Table 1. Flow cytometry staining

Analysis	Staining solution	Manufacturer
Cell cycle	0.2% Triton X-100, 0.5 mg/ml ribonuclease A and 0.025 mg/ml PI in 500 µl PBS)	Merck, Darmstadt, Germany
Phosphatidylserine (PS) externalization/PI	Annexin V-Alexa Fluor® 647 conjugate, PI	Thermo Scientific, Rockford, IL, USA
MMP (mitochondrial membrane potential)	TMRE (working solution: 0.1 µM TMRE)	Molecular Probes, Eugene, OR, USA
Caspase-3 (casp-3)	Active caspase-3-PE mAb	BD Biosciences Pharmingen, San Diego, CA, USA
Cleavage of PARP	Cleaved-PARP (Asp214) XP® Rabbit mAb (PE Conjugate)	Cell Signaling Technology, Danvers, MA, USA
Bcl-2	Bcl-2 (124) Mouse mAb (PE Conjugate)	
Phospho-Bcl-2	Phospho-Bcl-2 (Ser70) Rabbit mAb (Alexa Fluor® 488 Conjugate)	

Table 2. Primer sequences used in real-time PCR analysis

Gene	Forward primer	Reverse primer
ACTB (-actin)	5'-ACCAACTGGGACGACATGGAGAA-3'	5'-GTAGCCGCGCTCGGTGAGGATCT -3'
BAX	5´-CCCGAGAGGTCTTTTTCCGAG-3´	5´-CCAGCCCATGATGGTTCTGAT-3´
BCL2	5´-TCCATGTCTTTGGACAACCA-3´	5´-CCAGCCCATGATGGTTCTGAT-3´
BCL2L1 (Bcl-xL)	5´-TTACCTGAATGACCACCTA-3´	5´-ATTTCCGACTGAAGAGTGA-3´
CASP3	5´-TGGTTCATCCAGTCGCTTTG-3´	5´-CATTCTGTTGCCACCTTTCG-3´
CASP7	5´-AGTGACAGGTATGGGCGTTCG-3´	5´-GCATCTATCCCCCCTAAAGTGG-3´
CDKN1A (p21)	5'-GCAGACCAGCATGACAGATTT-3'	5'-GGATTAGGGCTTCCTCTTGGA-3'
CDKN1B (p27)	5'-AACGTGCGAGTGTCTAACGG-3'	5'-CCAGGAGTTACTTCTATGCCTGA-3'
PI3KCA	5´-CCTGATCTTCCTCGTGCTGCTC-3´	5´-ATGCCAATGGACAGTGTTCCTCTT-3´
AKT1	5'-GCAGCACGTGTACGAGAAGA-3'	5'-GGTGTCAGTCTCCGACGTG-3'
NFKBIA (IκB)	5'-GCAATTTCTGGCTGGTTGG-3'	5'-GATCCGCCAGGTGAAGGG-3'
CDK2	5'-GCTAGCAGACTTTGGACTAGCCAG-3'	5'-AGCTCGGTACCACAGGGTCA -3'
MAPK14 (p38)	5'-GCCGAGCTGTTGACTGGAAG-3'	5'-GGAGGTCCCTGCTTTCAAAGG-3'
APAF1	5'-TCCATGTATGGTGACCCATCC -3'	5'-AAGGTGGAGTACCACAGAGG-3'

Western Blot p21 and p27

Proteins were extracted from HeLa cells using a Laemmle buffer (1 mol/l Tris/HCl (pH = 7.4), glycerol, 20% SDS (sodium dodecyl sulfate), deionized H_2O) in the presence of protease inhibitors. Protein quantification was determined by the Pierce® BCA Protein Assay Kit (Thermo Scientific, Rockford, IL, United States) and measured using an automated Cytation™ 3 Cell Imaging Multi-Mode Reader (Biotek, Winooski, VT, USA) at wavelength 570 nm. The proteins were separated on SDS-PAA gel (12%) and transferred to a polyvinylidene difluoride (PVDF) membrane (GE Healthcare, Chicago, IL, United States) using the iBlotTM 2 dry blotting system (Thermo Scientific, Rockford, IL, United States). The membrane was blocked in 5% non-fat dry milk and incubated with primary antibodies p21 Waf/Cip1 and p27 (dilution of 1 : 1000, Cell Signaling Technology®, Danvers, Massachusetts, USA) at 4 °C overnight. The membrane was washed in TBS-Tween and incubated with the corresponding horseradish peroxidase (HRP)-conjugated secondary antibody (1 : 1000 dilution, Cell Signaling). The expression of proteins in the washed membrane was detected using a chemiluminescent ECL substrate (Thermo Scientific, Rockford, IL, United States) and MF-ChemiBIS 2.0 Imaging System (DNR BIO-Imaging Systems, Jerusalem, Israel). The detected band was analyzed densitometrically using the ImageJ free software. Equal loading was verified using the antibody against β-actin.

Immunocytochemistry

Treated HeLa cells (1×10^6) with KP7 (2 µM) for 24, 48, and 72 h were washed with 1 × PBS. Cytospins were produced using StatSpin Cytofuge 2 (Beckman Coulter, Atlanta, GA, USA). The cytospin slides were air-dried at room temperature and immunocytochemically stained by the EnVision FLEX System (Agilent, Santa Clara, CA, USA). Primary antibodies p21 (p21WAF1 / Cip1, Monoclonal Mouse Anti-Human, Clone SX118; dilution 1 : 50) and p27 (Monoclonal Mouse Anti-Human p27Kip1, Clone SX53G8; dilution 1 : 50) with counterstaining by hematoxylin were used for immunocytochemical detection. A light microscope Olympus BX40 F4 (Tokyo, Japan) and Olympus E 420 QuickPHOTO Industrial software were used for detection and documentation.

Statistical analysis

The results are expressed as mean ± SD. The significance of differences of means among more than two groups of continuous data was tested using one-way ANOVA followed by the Bonferroni procedure for multiplicity-corrected pairwise comparison tests. Values of $p < 0.05$ were considered to be statistically significant.

Results

MTT assay

Survival of HeLa cells exposed to KP7 in concentrations 0.5–10 μM for 72 h is shown in Fig. 1. Our data showed that homospisulosine (KP7) displayed appreciable dose-dependent antiproliferative activity with IC_{50} = 1.50 μM (CI95: 0.94–2.15 μM). Therefore, a 2 μM was used for further experiments in HeLa cells.

Flow cytometry

Analysis of cell cycle

To evaluate the effect of KP7 treatment on HeLa cell cycle progression, we performed flow cytometric analysis on cells treated with KP7 (2 μM) for 24, 48, and 72 h. After 48 h of incubation, cell cycle analysis found a significant increase in the proportion of events in the sub-G_0/G_1 subpopulation considered as apoptotic with fragmented DNA. Furthermore, the proportion of events in the sub-G_0/G_1 subpopulation increased with prolonged incubation time. In addition, G_2/M was also observed at 24 and 48 h after KP7 treatment. These findings suggest significant changes in cell cycle progression and induction of apoptosis (Table 3, Fig. 2).

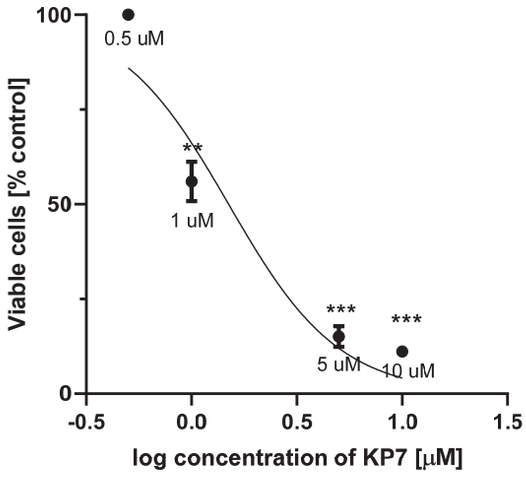

Fig. 1. The effects of KP7 on the number of viable HeLa cells after 72 h of incubation (based on the MTT test). Error bars: SD; Dose-response curve was fitted with Hill's model with normalized response and variable slope. Significance: ** $p < 0.01$, *** $p < 0.001$ vs untreated control set as 100%. IC_{50} = 1.50 μM (Hill's slope = −1.654).

Table 3. The effects of KP7 (2 μM) on the cell cycle in HeLa cells after 24, 48, and 72 h of incubation (in %)

	sub-G_0/G_1		G_0/G_1		S		G_2/M	
	CTRL	KP7	CTRL	KP7	CTRL	KP7	CTRL	KP7
24 h	1.89 (±0.35)	4.80 (±0.80)	74.41 (±6.63)	58.01 (±0.70)*	10.73 (±1.32)	18.20 (±2.30)	12.95 (±5.12)	19.01 (±1.80)*
48 h	1.68 (±0.35)	12.60 (±2.10)*	76.08 (±4.89)	43.70 (±3.10)**	10.61 (±1.09)	24.20 (±3.00)	11.62 (±3.97)	19.50 (±1.40)*
72 h	1.96 (±0.72)	28.70 (±1.70)**	76.07 (±4.91)	41.30 (±3.60)**	10.50 (±0.94)	18.60 (±2.50)	11.46 (±3.88)	11.50 (±1.20)

Note: The results of three independent experiments are presented as the mean ± SD; * $p < 0.05$, ** $p < 0.01$ indicate significant differences between treated vs untreated cells (control).

Apoptosis detection via externalized phosphatidylserine

Externalization of phosphatidylserine, which is normally localized on the internal surface of the lipid bilayer of the plasma membrane, occurs in the early stage of apoptosis and can be detected by the Annexin V-Alexa Fluor® 647 conjugate. The later stage of apoptosis is accompanied by loss of integrity of the cell membrane, which becomes permeable for PI. KP7 (2 μM) induced a significant increase in the proportion of apoptotic cells (An^+/PI^-) after 24 h treatment, followed by a further increase after 48 and 72 h. In addition, after 48 and 72 h treatment, a significant increase was observed in the proportion of Annexin V-positive/PI-positive cells that represent late apoptotic and/or secondarily necrotic cells (Table 4, Fig. 3).

Analysis of changes in MMP and dynamics of proteins in mitochondria

Activation of the internal mitochondrial apoptotic pathway reduces the mitochondrial membrane potential. We assessed the change in the mitochondrial membrane using the TMRE dye (tetramethylrhodamine ethyl ester perchlorate), a highly specific probe for detecting changes in mitochondrial membrane potential. In our experiment, we noticed a significant increase in the proportion of HeLa cells with reduced mitochondrial membrane potential after 24 h exposition with KP7 (2 μM), and this effect persisted for up to 72 h (Fig. 4A).

Analysis of Bcl2/phospho-Bcl2, caspase-3, and PARP by flow cytometry

Our analysis found that Bcl-2 was released in the cytoplasm, phosphorylated, and deactivated. Therefore, it could not mediate the anti-apoptotic effect (Fig. 4B).

Executioner caspase-3 is a protease frequently activated during apoptosis and primarily responsible for the cleavage of PARP (Poly (ADP-ribose) polymerase). Our flow cytometric analysis has shown significantly higher levels of caspase-3 (Fig. 4C) and its cleaved substrate PARP (Fig. 4D) in HeLa cells treated with KP7 (2 μM) for 48 and 72 h.

Quantitative real-time PCR

The cell cycle analysis showed that KP7 (2 μM) induces a significant increase of HeLa cells in the sub-G_0/G_1 population, considered an apoptotic subpopulation with fragmented DNA. To verify whether the induction of apoptosis is associated with changes in gene expression on the mRNA level, we conducted quantitative real-time PCR analysis for selected pro-apoptotic and anti-apoptotic genes. Data has shown a significant increase in AKT1, caspase-3, CDK2, p21, and p27 gene expression on mRNA level after 24 h of treatment. The upregulation of caspase-3, CDK2, and p27 persisted at 48 h of treatment (Table 5).

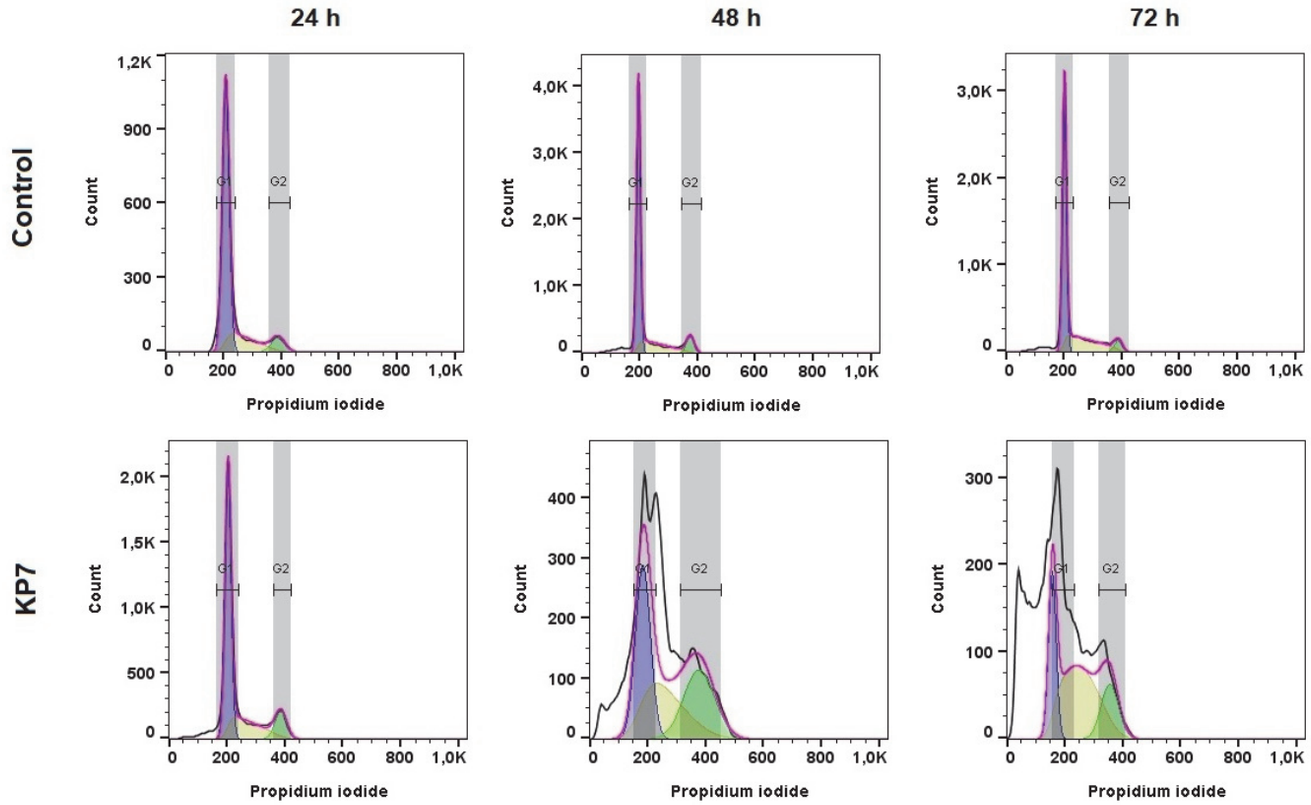

Fig. 2. Flow cytometry analysis of cell cycle of HeLa cells treated with control or KP7 for 24, 48, and 72 hours. The images present representative data and analysis of a single flow cytometry experiment that was replicated 3 times (for summary data see Table 3). Black curves: distribution of PI fluorescence events originally recorded in the flow cytometry experiment (after discrimination of doublets); Blue area: modelled sub-population of G1 cells; Yellow area: modelled sub-population of S cells; green area: sub-population of G_2/M cells; violet curves: modelled distribution of cells.

Table 4. Annexin V/PI flow cytometry analysis of apoptosis occurrence in HeLa cells after KP7 (2 μM) treatment after 24 h, 48 h, and 72 h of incubation (in %)

	Live (An^-/PI^-)		Apoptosis (An^+/PI^-)		Late apoptosis / Sec. Necrosis (An^+/PI^+)		Necrosis (An^-/PI^-)	
	CTRL	KP7	CTRL	KP7	CTRL	KP7	CTRL	KP7
24 h	93.21 (±0.12)	77.76 (±6.86)*	0.33 (±0.35)	8.53 (±0.31)*	0.72 (±0.26)	3.04 (±3.29)	5.72 (±0.74)	10.66 (±3.88)*
48 h	88.72 (±6.22)	57.56 (±1.16)**	0.44 (±0.51)	14.61 (±1.45)**	2.41 (±2.65)	9.58 (±3.07)*	8.41 (±1.05)	18.22 (±3.05)*
72 h	61.63 (±7.78)	61.63 (±7.78)**	1.41 (±1.87)	21.96 (±5.33)**	0.65 (±0.16)	6.26 (±2.64)*	4.80 (±3.36)	10.13 (±0.19)*

Note: The results are presented from three independent experiments as the mean ± SD. * $p < 0.05$, ** $p < 0.01$ indicate significant differences between treated vs untreated cells (control).

Western blot

Western blot analysis revealed a significant time-dependent increase in p27 protein levels, which occurred after 24 hours of incubation with KP7 (2 μM) and continued to increase with increasing incubation time. In contrast, p21 levels did not display significant changes at 24 h and 72 h, but showed a significant decrease after 72 h of incubation (Fig. 5). These results are consistent with our gene expression analysis and subsequent immunocytochemistry analysis.

Immunocytochemistry

Immunocytochemical evaluation found increased levels of p27 in nuclei of HeLa cells treated with KP7 (2 μM). In contrast, no remarkable changes in staining intensity or cellular localization were observed for p21 (Fig. 6). Notably, nuclear localization and staining intensity of p27 are a significant findings, because it has been previously associated with pro-apoptotic effects, while cytoplasmic localization of p27 was reported to be anti-apoptotic (Blagosklonny, 2002).

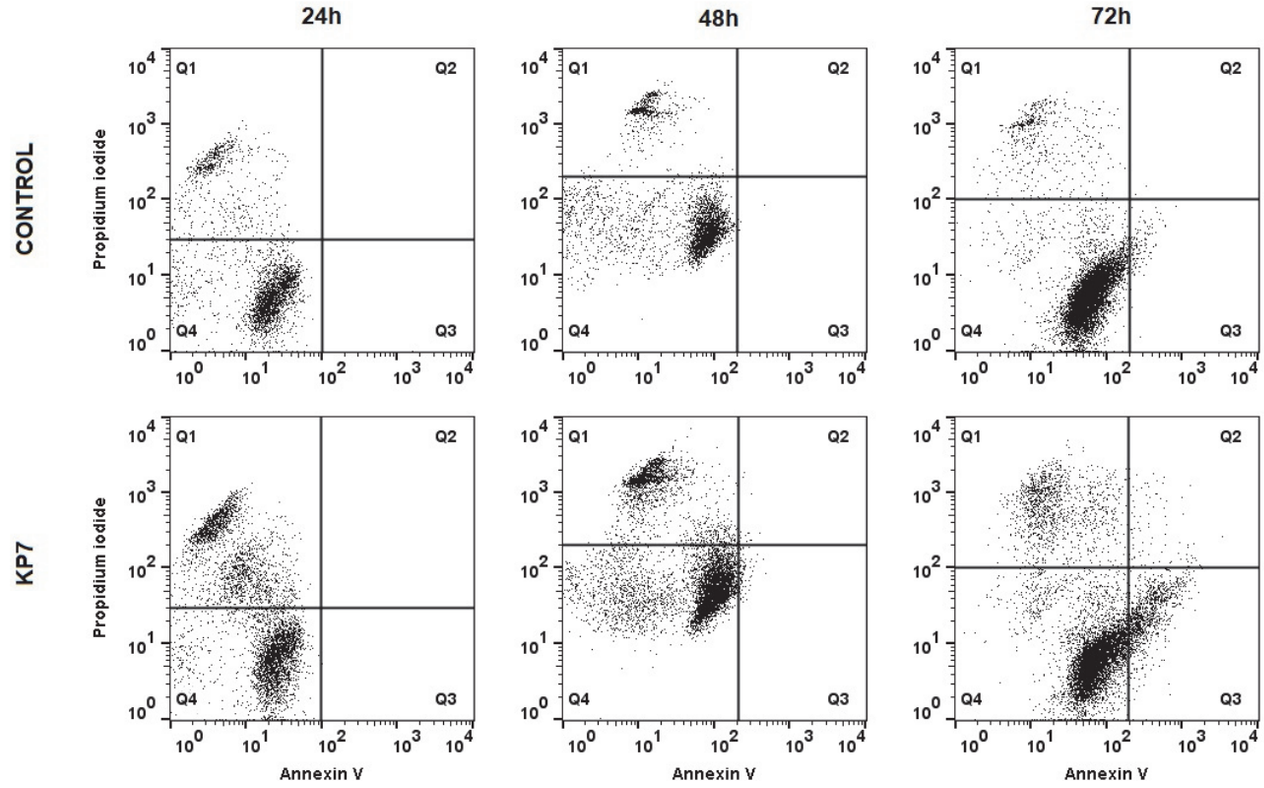

Fig. 3. The representative dot plot of Annexin V/PI analyses of HeLa cells treated with KP7 at 24, 48, and 72 h. Legend: Q4 = Live $An^{-}PI^{-}$, Q3 = Apoptotic $An^{+}PI^{-}$, Q2 = Late apoptotic $An^{+}PI^{+}$, Q1 = Death $An^{-}PI^{+}$.

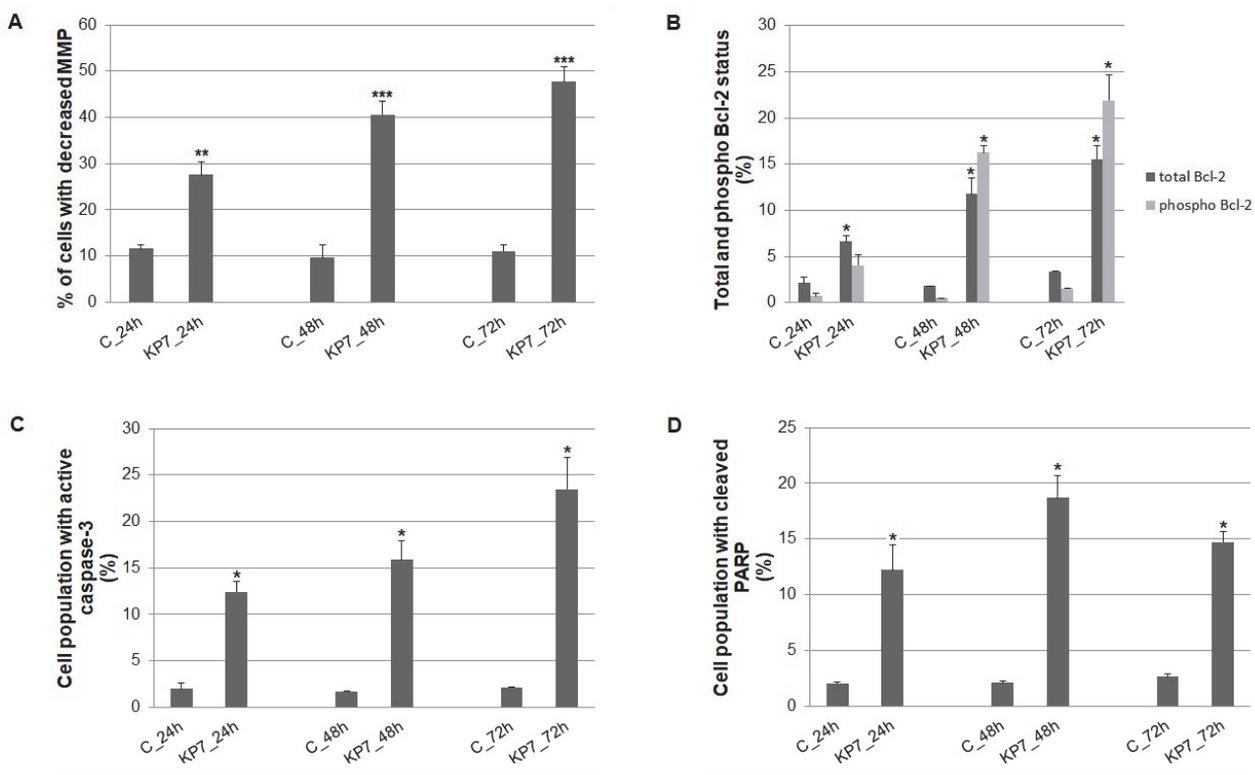

Fig. 4. Flow cytometric analysis of He; La cells after 24, 48, and 72 h of treatment with KP7 (2 μM). (**A**) mitochondrial membrane potential changes, (**B**) relative % levels of Bcl-2 and phospho Bcl-2 protein, (**C**) caspase-3 activation, (**D**) cleavage of PARP. The results are presented from three independent experiments as the mean ± SD values. * $p < 0.05$, ** $p < 0.01$, *** $p < 0.001$ indicate significant differences between treated vs untreated cells (control).

Table 5. Fold changes in gene expression level after treatment with KP7 (2 μM)

pro-apoptotic	Normalized ratio			*anti-apoptotic*	Normalized ratio		
	24 h	48 h	72 h		24 h	48 h	72 h
BAX	1.07	0.90	0.90	*PI3KCA*	0.84	1.20	0.78
CASP3	8.21***	2.76**	1.76*	*AKT1*	2.66**	1.57*	1.12
CASP7	0.80	0.96	1.21	*BCL2*	0.88	1.09	0.94
CDK2	2.46**	2.54**	1.34	*BCL2L1* (Bcl-xL)	1.17	0.96	1.22
MAPK14 (p38)	1.27	1.40	0.97	*NFKBIA* (IκB)	1.16	1.46	1.01
APAF	1.18	0.98	0.51				
				CDK inhibitors			
CDKN1B (p27)	2.47**	3.75**	1.51	*CDKN1A* (p21)	3.57**	1.22	0.89

Note: The results are presented from three independent experiments as the mean ± SD. * $p < 0.05$, ** $p < 0.01$, *** $p < 0.001$, that indicate significant differences between treated vs untreated cells (control).

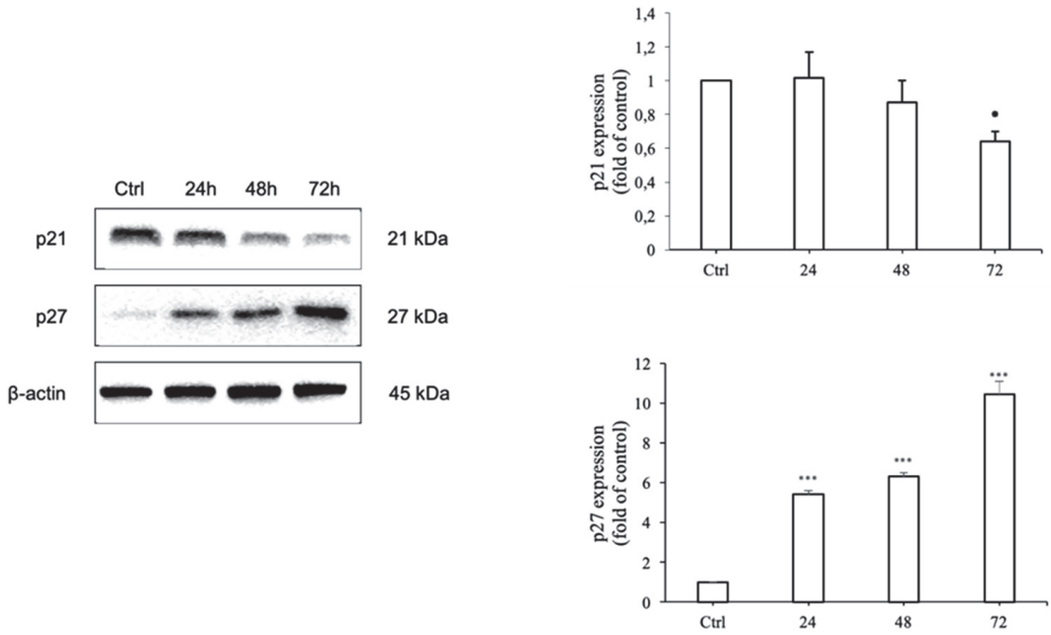

Fig. 5. Western blot analysis of p21 (21 kDa), p27 (27 kDa), and β-actin (42 kDa) in HeLa cell treated with KP7 (2 μM) for 24, 48, and 72 h. Bar graphs demonstrate densitometric quantification of band intensities normalized to β-actin. Significant differences: * $p < 0.05$, *** $p < 0.001$ vs untreated control.

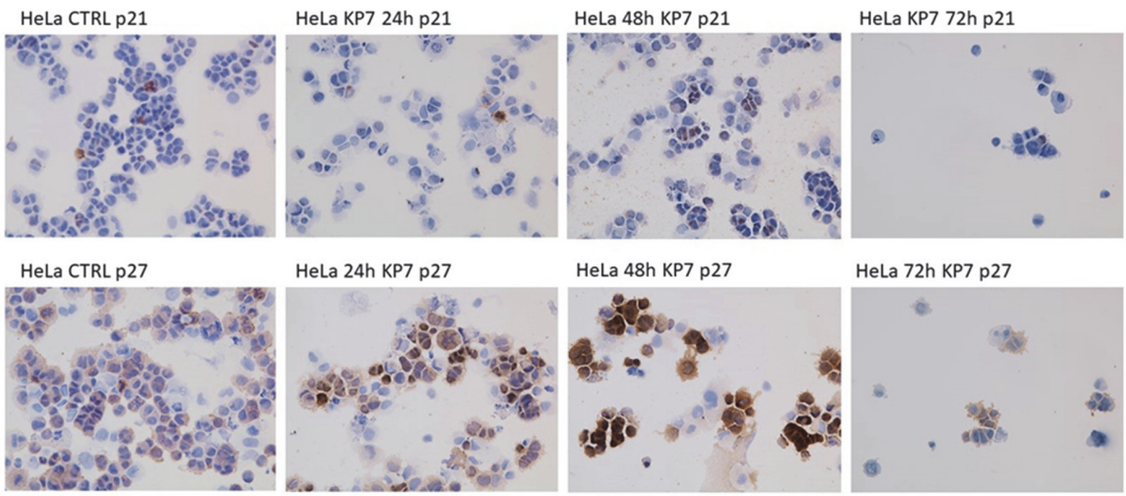

Fig. 6. Immunocytochemical detection of p21 and p27 in HeLa cells treated with KP7 (2 μM) for 24, 48, and 72 h. Magnification 100×.

Discussion

The seas and oceans are unimaginable sources of new substances with chemical and biological diversity and potential in cancer research (Chakraborty et al., 2009). These compounds with structural features generally not found in terrestrial natural products were isolated primarily from marine invertebrates, including sponges, soft corals, veggies, molluscs, and other marine organisms (Malve, 2016). Notably, marine products have been used for medical purposes in India, China, the Middle East, and Europe since ancient times (Sithranga Boopathy and Kathiresan, 2010).

Spisulosine (1-deoxysphinganine) is a sphingoid amino alcohol isolated from edible *Spisula polynyma* clam (Rinehart et al., 2000). Sphingoid bases form the backbone of sphingolipids, a group of specialized lipids that includes sphingomyelins, ceramides, cerebrosides, and gangliosides. Some of these biomolecules are crucial in cell signaling that controls cancer cell growth differentiation and apoptosis. For instance, ceramides, formed by the hydrolysis of ubiquitous cell membrane sphingomyelins, induce apoptosis and other forms of cancer cell deaths. However, ceramides can be metabolized by ceramidases to sphingosine and subsequently phosphorylated by sphingosine kinases to form sphingosine-1-phosphate (S1P), which inhibits ceramide-mediated apoptosis and supports cancer cell proliferation and resistance to anticancer drugs (Ogretmen, 2018).

Spisulosine (also known as ES 285) is a structural analog of sphingosine that was shown to inhibit human sphingosine kinase 1 (SPHK1) (National Library of Medicine, 2023) and suppress *in vitro* growth of cell lines representing a broad spectrum of solid tumors (Jimeno et al., 2004; Schöffski et al., 2011). The underlying mechanism of its action is not yet entirely understood; nevertheless, spisulosine reportedly induces an endoplasmic reticulum stress-dependent "atypical" apoptotic pathway that includes the activation of caspases-3 and -12, phosphorylation of p53, but not impaired mitochondrial integrity (Salcedo et al., 2007). Furthermore, cells exposed to spisulosine displayed concentration-dependent disassembly of actin stress fibers and rapid cell detachment *in vitro* followed by apoptosis but no observed changes in microtubules (Cuadros et al., 2000). Since these changes were partially preventable by treatment with sphingosine-1-phosphate (S1P) agonist LPA (lysophosphatidic acid), spisulosine likely induced these actin cytoskeleton changes through modulation of a small GTP-binding protein Rho signaling. Consequently, spisulosine can act as a partial agonist of S1P/LPA and impair cell adhesion and mobility, but these receptors are not essential for spisulosine-induced cell death (Cuadros et al., 2000). Notably, ERK, AKT, and JNK pathways were not found to play a major role in spisulosine-induced apoptosis of NIH-3T3 and RH7777 cells, of which the former express and latter do not express the LPA/S1P receptors (Cuadros et al., 2000).

To develop new spisulosine analogs with potentially more favorable activity and toxicity profiles, we evaluated the antiproliferative/cytotoxic activity and mode of action of homospisulosine (KP7). This structurally close spisulosine analog displayed a significant antiproliferative/cytotoxic effect on five different cancer cell lines (IC_{50} < 10 μM) with higher potency than the traditional anticancer drugs cisplatin and topotecan on three of the five cancer cell lines tested in our previous study (Stanková et al., 2015). In our test, KP-7 also displayed a higher potency than the traditional anticancer drugs cisplatin and etoposide on three of the five cancer cell lines tested in our previous study (Stanková et al., 2015).

We are particularly interested in developing anticancer drugs for cervical carcinomas, which were not included in our panel of five cancer cell lines. Our interest stems from the challenges posed by locally advanced and metastatic cervical carcinomas to traditional chemotherapy-containing treatment modalities (Burmeister et al., 2022), and especially by cervical adenocarcinomas represented by HeLa cells, which typically show even poorer response to treatment than squamous cell carcinomas (Katanyoo et al., 2012). For these reasons, we expanded our previous panel of five tested cancer cell lines by including the HeLa cervical adenocarcinoma cell line in the original panel. Interestingly, KP-7 demonstrated higher antiproliferative/cytotoxic potency in this study on HeLa cells than on the five other cancer cell lines used in our previous study (Stanková et al., 2015), of which the most responsive to KP7 was the CaCO-2 cell line with IC_{50} ± SD of 2,2 ± 1.7 μM. The antiproliferative/cytotoxic effect of KP7 was also evaluated on non-malignant murine NIH 3T3 cells that represent spontaneously immortalized and tetraploid fibroblasts, yielding an IC_{50} ± SD of 4.3 ± 1.3 μM (Leibiger et al., 2013; Stanková et al., 2015) (Suppl. 1).

Furthermore, in comparison with the Genomics of Drug Sensitivity in Cancer (GDSC2) data generated for a 72-hour resazurin-based test (Yang et al., 2013), homospisulosine demonstrated lower potency in HeLa cells than docetaxel (2.7 nM), gemcitabine (IC_{50} = 91 nM), and doxorubicin (IC_{50} = 236 nM); comparable potency to that of etoposide (IC_{50} =1.2 uM), and higher potency than cisplatin (IC_{50} = 25 uM) and 5-fluorouracil (IC_{50} = 106 uM).

Based on these results, we further evaluated the ability of KP7 to induce apoptosis in HeLa cells and molecular mechanisms that may be involved in this process. Our analysis of cell cycle distribution revealed a significant increase in the HeLa sub-G_0/G_1 cell population after 48 h, which increased with a prolonged time of incubation and G_2/M arrest. These data suggest the ability of KP7 to induce apoptosis detected by fragmentation and loss of the cellular DNA. The apoptosis-inducing effect of KP7 was further confirmed by flow cytometric detection of externalized phosphatidylserine, activation of caspase-3, and cleavage of its target PARP protein. In contrast to the previously reported mode of apoptosis induced by spisulosine, which included endoplasmic reticulum stress-mediated process without impaired mitochondrial integrity (Salcedo et al., 2007), our results for its close analog homospisulosine support dissipation of mitochondrial membrane potential, which is linked to the formation of mitochondrial permeability transition (PT) pores (Zamzami et al., 1996).

Our data also show increased phosphorylation of Bcl-2 in spisulosine-treated HeLa cells. Prior research identified the conflicting role of Bcl-2 phosphorylation in regulating apoptosis. For instance, some investigators suggested phosphorylation on Ser70 is necessary for its anti-apoptotic function (Ito et al., 1997). In contrast, however, others suggested the importance of Bcl-2 phosphorylation for the induction of apoptosis in cancer cells by paclitaxel (Haldar et al., 1996). Our results indicate up-regulation of Bcl-2 on the protein level and its extensive phosphorylation in cells treated with homospisulosine, which implies phosphorylation-mediated inhibition of anti-apoptotic function of Bcl-2 in the context of our study. Taken together, our results support the loss of the mitochondrial membrane potential associated with phosphorylation-inactivated Bcl-2 in homospisulosine-treated Hela cells, which differs from previously reported findings for spisulosine (Salcedo et al., 2007). These differences may reflect existing mechanistic differences between spisulosine and homospisulosine, or biological differences between HeLa cells and hepa-

toma cells/fibroblasts used in the spisulosine and homospisulosine studies, respectively.

Our results also demonstrate protein levels down-regulation of p21 (CDKN1A) at 72 hours and up-regulation of p27 (CDKN1B) at all study time points. These two cyclin-dependent kinases (CDKs) inhibitors have been implicated in the development and progression of many malignancies with conflicting roles depending on cell context (Abukhdeir and Park, 2008). Since p21 can increase the resistance of cancer cells to apoptosis (Blagosklonny, 2002), our finding of decreased levels of p21 in homospisulosine-treated HeLa cells is consistent with observed apoptosis in these cells. Intriguingly, increased levels of p27 were previously associated with apoptotic cell death induced in PC-3 prostate cancer cells by ceramide, a sphingolipid with a sphingoid base structurally similar to that of homospisulosine. As a result, the upregulation of p27 is likely mechanistically relevant to homospisulosine-induced apoptosis in HeLa cells (Kim et al., 2010). Although p21 is primarily known for its ability to inhibit cancer cell proliferation, it can also prevent apoptosis, which may explain its unexpected oncogenic properties as discussed in a review article by Abbas and Dutta (2009). Several mechanisms can counteract p21's ability to arrest the cell cycle and inhibit apoptosis, including selective transcriptional repression of the CDKN1A gene encoding p21, activation of proapoptotic genes, or post-translational modifications of p21 (such as its phosphorylation or cleavage by caspase 3). In cells treated with KP-7 for 72 hours, these mechanisms may lead to the observed decrease of p21 on protein level and promote apoptosis instead of cell cycle arrest and senescence.

Conclusion

Homospisulosine is a new analog of a marine natural product, spisulosine, which was previously evaluated as an investigational anticancer drug in Phase I clinical trial. Considering the need to develop new analogs of spisulosine with better activity and safety profiles, we have synthesized and evaluated the anticancer activity of homospisulosine *in vitro*. Taken together, we found that homospisulosine inhibits the proliferation of various cancer cells with appreciable potency. Our previous finding that homospisulosine (KP-7) has significant antiproliferative/cytotoxic effects on murine non-tumor NIH 3T3 fibroblasts may appear to be a limitation for the future development of this promising compound. Nevertheless, NIH 3T3 cells do not entirely represent non-cancer cells that can be used as a universal reference for the evaluation of unintended cytotoxicity against non-cancer cells since these cells are spontaneously immortalized and tetraploid, which distances them further from non-cancer cells. We plan to evaluate the toxicity of homospisulosine in a future dedicated study using HUVEC cells and stem cell cultures committed to specific differentiation lineages that would serve as better predictors of toxicity.

Our finding that homospisulosine induces apoptosis associated with phosphorylation of Bcl-2 and upregulation of p27 suggests its mechanistic similarity with structurally similar ceramide, a well-known inducer of apoptosis whose analogs are investigated for anticancer drug development. Our results support the relevance of spisulosine analogs represented here by homospisulosine for future drug development.

Data availability statement

The data presented in this study can be provided by the authors on reasonable request.

Funding

This research was funded by the Slovak Grant Agency for Science VEGA No 1/0278/23, VEGA No 1/0539/21 and VEGA No 1/0653/19. This publication is also the result of the project: "Open scientific community for modern interdisciplinary research in medicine (OPENMED)", ITMS2014+: 313011V455, supported by the Operational Programme Integrated Infrastructure, funded by the ERDF.

Author contributions

M.B.P., R.M., and M.K. wrote the paper, and designed and supervised the experiments; M.K. and G.O. performed and analyzed flow cytometry data; P.T., N.N. and M.B.P. performed RT-PCR; K.K. and N.N. performed and analyzed Western blot data; P.P., N.N. and P.B. performed immunocytochemistry experiments; M.M. and K.S. performed the synthesis and characterization; M.K. and M.M. provided financial support; R.M. reviewed and interpreted the data; R.M. and M. B. P. responded to reviewer's comments and revised the manuscript; M.K. and R.M. contributed to supervising all parts of the work and approved the final version of the manuscript. R.M. responded to the reviewer's comments. All authors have read and agreed to the published version of the manuscript.

Ethical aspects and conflict of interest

The authors have no conflict of interest to declare.

References

Abbas T, Dutta A (2009). p21 in cancer: intricate networks and multiple activities. Nat Rev Cancer 9(6): 400–414. DOI: 10.1038/nrc2657.

Abukhdeir AM, Park BH (2008). P21 and p27: roles in carcinogenesis and drug resistance. Expert Rev Mol Med 10: e19. DOI: 10.1017/S1462399408000744.

Baird RD, Kitzen J, Clarke PA, Planting A, Reade S, Reid A, et al. (2009). Phase I safety, pharmacokinetic, and pharmacogenomic trial of ES-285, a novel marine cytotoxic agent, administered to adult patients with advanced solid tumors. Mol Cancer Ther 8(6): 1430–1437. DOI: 10.1158/1535-7163.MCT-08-1167.

Blagosklonny MV (2002). Are p27 and p21 cytoplasmic oncoproteins? Cell Cycle 1(6): 391–393. DOI: 10.4161/cc.1.6.262.

Burmeister CA, Khan SF, Schafer G, Mbatani N, Adams T, Moodley J, Prince S (2022). Cervical cancer therapies: Current challenges and future perspectives. Tumour Virus Res 13: 200238. DOI: 10.1016/j.tvr.2022.200238.

Chakraborty C, Hsu CH, Wen ZH, Lin CS (2009). Anticancer drugs discovery and development from marine organism. Curr Top Med Chem 9(16): 1536–1545. DOI: 10.2174/156802609789909803.

Cuadros R, Montejo de Garcini E, Wandosell F, Faircloth G, Fernandez-Sousa JM, Avila J (2000). The marine compound spisulosine, an inhibitor of cell proliferation, promotes the disassembly of actin stress fibers. Cancer Lett 152(1): 23–29. DOI: 10.1016/s0304-3835(99)00428-0.

Den Brok MW, Nuijen B, Garcia JL, Miranda E, Calvo P, Manada C, Beijnen JH (2006). Compatibility and stability of the novel anticancer agent ES-285 x HCl formulated with 2-hydroxypropyl-beta-cyclodextrin in infusion devices. Pharmazie 61(1): 21–24.

Den Brok MW, Nuijen B, Meijer DM, Millan E, Manada C, Beijnen JH (2005). Pharmaceutical development of a parenteral lyophilised formulation of the investigational anticancer agent ES-285.HCl. PDA J Pharm Sci Technol 59(4): 246–257.

Haefner B (2003). Drugs from the deep: marine natural products as drug candidates. Drug Discov Today 8(12): 536–544. DOI: 10.1016/s1359-6446(03)02713-2.

Haldar S, Chintapalli J, Croce CM (1996). Taxol induces bcl-2 phosphorylation and death of prostate cancer cells. Cancer Res 56(6): 1253–1255.

Ito T, Deng X, Carr B, May WS (1997). Bcl-2 phosphorylation required for anti-apoptosis function. J Biol Chem 272(18): 11671–11673. DOI: 10.1074/jbc.272.18.11671.

Jimeno J, López-Martín JA, Ruiz-Casado A, Izquierdo MA, Scheuer PJ, Rinehart K (2004). Progress in the clinical development of new marine-derived anticancer compounds. Anticancer Drugs 15(4): 321–329. DOI: 10.1097/00001813-200404000-00003.

Katanyoo K, Sanguanrungsirikul S, Manusirivithaya S (2012). Comparison of treatment outcomes between squamous cell carcinoma and adenocarcinoma in locally advanced cervical cancer. Gynecol Oncol 125(2): 292–296. DOI: 10.1016/j.ygyno.2012.01.034.

Kim SW, Kim HJ, Chun YJ, Kim MY (2010). Ceramide produces apoptosis through induction of p27(kip1) by protein phosphatase 2A-dependent Akt dephosphorylation in PC-3 prostate cancer cells. J Toxicol Environ Health A 73(21–22): 1465–1476. DOI: 10.1080/15287394.2010.511553.

Lefever S, Vandesompele J, Speleman F, Pattyn F (2009). RTPrimerDB: the portal for real-time PCR primers and probes. Nucleic Acids Res 37(Database issue): D942–945. DOI: 10.1093/nar/gkn777.

Leibiger C, Kosyakova N, Mkrtchyan H, Glei M, Trifonov V, Liehr T (2013). First molecular cytogenetic high resolution characterization of the NIH 3T3 cell line by murine multicolor banding. J Histochem Cytochem 61(4): 306–312. DOI: 10.1369/0022155413476868.

Malve H (2016). Exploring the ocean for new drug developments: Marine pharmacology. J Pharm Bioallied Sci 8(2): 83–91. DOI: 10.4103/0975-7406.171700.

Mosmann T (1983). Rapid colorimetric assay for cellular growth and survival: application to proliferation and cytotoxicity assays. J Immunol Methods 65(1–2): 55–63. DOI: 10.1016/0022-1759(83)90303-4.

National Library of Medicine. National Center for Biotechnology Information (2023). PubChem Compound Summary for CID 9925886, Spisulosine. [online] [cit. 2023-01-22]. Available from: https://pubchem.ncbi.nlm.nih.gov/compound/Spisulosine

Ogretmen B (2018). Sphingolipid metabolism in cancer signalling and therapy. Nat Rev Cancer 18(1): 33–50. DOI: 10.1038/nrc.2017.96.

Rinehart KL, Fregeau NL, Warwick RA (2000). Spisulosine compounds. Google Patents. [online] [cit. 2023-01-22]. Available from: https://patents.google.com/patent/US20040147615A1/en

Rios Ade O, Antunes LMG, Bianchi, MdLP (2009). Bixin and lycopene modulation of free radical generation induced by cisplatin-DNA interaction. Food Chem 113(4): 1113–1118. DOI: 10.1016/j.foodchem.2008.08.084.

Roginsky AB, Ujiki MB, Ding XZ, Adrian TE (2005). On the potential use of flavonoids in the treatment and prevention of pancreatic cancer. In Vivo 19(1): 61–67.

Salcedo M, Cuevas C, Alonso JL, Otero G, Faircloth G, Fernandez-Sousa JM, et al. (2007). The marine sphingolipid-derived compound ES 285 triggers an atypical cell death pathway. Apoptosis 12(2): 395–409. DOI: 10.1007/s10495-006-0573-z.

Sánchez AM, Malagarie-Cazenave S, Olea N, Vara D, Cuevas C, Díaz-Laviada I (2008). Spisulosine (ES-285) induces prostate tumor PC-3 and LNCaP cell death by de novo synthesis of ceramide and PKCzeta activation. Eur J Pharmacol 584(2-3): 237–245. DOI: 10.1016/j.ejphar.2008.02.011.

Schöffski P, Dumez H, Ruijter R, Miguel-Lillo B, Soto-Matos A, Alfaro V, Giaccone G (2011). Spisulosine (ES-285) given as a weekly three-hour intravenous infusion: results of a phase I dose-escalating study in patients with advanced solid malignancies. Cancer Chemother Pharmacol 68(6): 1397–1403. DOI: 10.1007/s00280-011-1612-1.

Singh R, Sharma M, Joshi P, Rawat DS (2008). Clinical status of anti-cancer agents derived from marine sources. Anticancer Agents Med Chem 8(6): 603–617.

Sithranga Boopathy N, Kathiresan K (2010). Anticancer drugs from marine flora: an overview. J Oncol 2010: 214186. DOI: 10.1155/2010/214186.

Stanková K, Martinková M, Gonda J, Bago M, Pilátová M, Gönciová G (2015). The convergent total synthesis of cytotoxic homospisulosine and its 3-epi-analogue. Tetrahedron: Asymmetry 26(24): 1394–1407. DOI: 10.1016/j.tetasy.2015.11.001.

Vilar E, Grünwald V, Schöffski P, Singer H, Salazar R, Iglesias JL, et al. (2012). A phase I dose-escalating study of ES-285, a marine sphingolipid-derived compound, with repeat dose administration in patients with advanced solid tumors. Invest New Drugs 30(1): 299–305. DOI: 10.1007/s10637-010-9529-9.

Yang W, Soares J, Greninger P, Edelman EJ, Lightfoot H, Forbes S, et al. (2013). Genomics of Drug Sensitivity in Cancer (GDSC): a resource for therapeutic biomarker discovery in cancer cells. Nucleic Acids Res 41(Database issue): D955–961. DOI: 10.1093/nar/gks1111.

Zamzami N, Marchetti P, Castedo M, Hirsch T, Susin SA, Masse B, Kroemer G (1996). Inhibitors of permeability transition interfere with the disruption of the mitochondrial transmembrane potential during apoptosis. FEBS Lett 384(1): 53–57. DOI: 10.1016/0014-5793(96)00280-3.